Lithos 120 (2010) 14–29

Contents lists available at ScienceDirect

Lithos

journal homepage: www.elsevier.com/locate/lithos

Europe from the bottom up: A statistical examination of the central and northern European lithosphere–asthenosphere boundary from comparing seismological and electromagnetic observations

Alan G. Jones [a,*], Jaroslava Plomerova [b], Toivo Korja [c], Forough Sodoudi [d], Wim Spakman [e]

[a] Dublin Institute for Advanced Studies, 5 Merrion Square, Dublin 2, Ireland
[b] Geophysical Institute, Czech Academy of Sciences, 141 31 Prague 4, Czech Republic
[c] Geophysics Group, Department of Physical Sciences, University of Oulu, P.O.B. 3000, FI-90014, Oulu, Finland
[d] Helmholtz Centre Potsdam, GFZ German Research Centre for Geosciences, Telegrafenberg, 14473 Potsdam, Germany
[e] Department of Earth Sciences, Faculty of Geosciences, Utrecht University, P.O. box 80021, 3508 TA Utrecht, The Netherlands

ARTICLE INFO

Article history:
Received 12 October 2009
Accepted 19 July 2010
Available online 24 July 2010

Keywords:
Lithosphere–asthenosphere boundary (LAB)
Europe
Seismology
Magnetotellurics

ABSTRACT

The Lithosphere–Asthenosphere Boundary (LAB) is a fundamental boundary in the plate tectonic paradigm — it is the most pervasive on the planet, yet comparatively it is one we know little about. Defined initially on the basis of the mechanical response of the Earth to loading, its usage has become ubiquitous across the geosciences but the natural differences in its definition, due to differences in thermal, physical and chemical parameters, cause confusion. To advance this debate, comparisons are made both qualitatively and quantitatively, between the delineation of the LAB for Europe based on seismological and electromagnetic observations. We examine statistically, using robust methods, the LABs derived from independent datasets and methods.

Essentially, all definitions of the LAB, as an impedance contrast from receiver functions (sLABrf), a seismic anisotropy change (sLABa) and an increase in conductivity from magnetotellurics (eLAB), are consistent with a deeper LAB beneath Precambrian Europe, and a shallower LAB beneath Phanerozoic Europe, with some exceptionally deep regions in Phanerozoic Europe, such as the Alps. All three LABs increase in depth significantly and rapidly at a location consistent with the surface expression of the Trans-European Suture Zone (TESZ) which separates Precambrian Europe to the north and east from Phanerozoic Europe in the centre. Two of the definitions, sLABrf and eLAB, are consistent for Phanerozoic Europe with mean values of 90–100 km, compared to an average sLABrf of 135 km. A different two, sLABa and sLABrf, are consistent for Precambrian Europe with mean values of 170–180 km compared to an eLAB mean of 250 km. The deeper eLAB depths for Precambrian Europe are more consistent with body wave and surface wave tomography models than are the sLABa and sLABrf ones, suggesting that the lower lithosphere beneath Precambrian Europe between 170 to 250 km is responding to shearing on the base of the lithosphere from plate driving forces.

Taken together the definitions provide strong constraints on the nature of the LAB. For example, the electrical eLAB beneath the TESZ is anomalously thick, to possibly the transition zone, whereas sLABa and sLABrf seismological definitions would place it at far shallower depths. Given the sensitivity of electrical conductivity to partial melt and water content, the thick eLAB beneath the TESZ excludes interpretation of the seismic LAB in that location in terms of a thermal structure that would induce partial melting or of hydration.

1. Introduction

The boundary between the Lithosphere and Asthenosphere, the LAB, is a fundamental boundary in the plate tectonic paradigm separating the rigid material of the plates from ductile convecting material below on which the plates ride. It is the most extensive on the planet, exists beneath both oceans and continents, yet perversely it is the boundary that comparatively we know little about (Eaton et al., 2009; Romanowicz, 2009; Fischer et al., 2010), but when discussed is one that is too readily assumed to be understood. The difficulty of its identification is compounded by the different geophysical and geochemical proxies used (Eaton et al., 2009), all of which are sensitive to variations in different physical or chemical

* Corresponding author.
E-mail addresses: alan@cp.dias.ie (A.G. Jones), jpl@ig.cas.cz (J. Plomerova), toivo.korja@oulu.fi (T. Korja), forough@gfz-potsdam.de (F. Sodoudi), wims@geo.uu.nl (W. Spakman).

0024-4937/$ – see front matter © 2010 Elsevier B.V. All rights reserved.
doi:10.1016/j.lithos.2010.07.013

properties. Certainly, the recent global compilation of the depth to the LAB based on imaging P-to-S converted phases by Rychert and Shearer (2009) with an "LAB" at 95 ± 4 km beneath Precambrian regions is seriously at odds with almost all other geophysical definitions and with petrological observations, highlighting the problem of definitive attribution of a boundary to an imaged geophysical or geochemical interface.

Artemieva (2009) recently provided an excellent summary of the different types of LAB, with three broad definitions in terms of a Mechanical Boundary Layer (MBL), a Thermal Boundary Layer (TBL) and a Chemical Boundary layer (CBL, or geochemically-defined Continental Lithosphere, CL, (Anderson, 1995)). Generally, the MBL is about half the thickness of the other two (Artemieva, 2009), and on occasion the TBL and CBL concur. However, the CBL can exhibit spatially rapid depth variations which are inherently excluded in any TBL observations as the thermal field naturally is diffusive in nature and strong lateral thermal contrasts can only be maintained on geologically short time-scales.

To further our understanding of the nature of the LAB and of the inter-relationships between some of the various geophysical proxies, we compare and contrast depths to the LAB derived from seismological and electromagnetic observations across Europe. This paper is not intended to be an exhaustive review of the LAB beneath Europe, but rather an objective comparison of estimates of depths to the LAB and their inter-relationships, using robust statistical techniques, from two seismological methods and from magnetotellurics (MT). As such, we view our work as the first step in what must become a global effort to compare and contrast LAB estimates from a multitude of techniques if we are to further our understanding of the nature of the LAB.

Begging the question of the nature of the LAB is our definitions of the *lithosphere* and *asthenosphere* themselves, without which we cannot define the LAB. Generally, for the purpose of our comparison we define the lithosphere as (cold) electrically resistive, seismically fast material with an anisotropy direction often different from present-day absolute plate motion (APM), whereas the asthenosphere is (hot) electrically conductive, seismically slow material with an anisotropy direction parallel to APM (e.g., Eaton et al., 2009). The techniques we use to image the Earth employ seismic and electromagnetic waves, and are thus primarily sensitive to strong temperature variation (e.g., Jones et al., 2009), so we are generally imaging the depth to the TBL, rather than to the MBL or CBL.

Fig. 1 shows a generalized age domain map of Europe from Artemieva (pers. comm.). The dominant tectonic feature of Europe, besides the topographic feature of the Alps, is the Trans-European Suture Zone (TESZ) that separates predominantly Phanerozoic Europe to the southwest from predominantly Precambrian Europe to the northeast. The TESZ is a fundamental boundary in the LAB that shows up in all of the proxies, albeit with differing estimates of the contrasting depths to the LAB across it, and the rapid change in the depth to the LAB has been observed in many geophysical studies, particularly as part of focussed seismological and electromagnetic experiments of the TESZ, e.g., TOR, CEMES, POLONAISE and CELEBRATION (e.g., Gregersen et al., 2002; Plomerova et al., 2002a; Guterch and Grad, 2006; Pushkarev et al., 2007; Semenov et al., 2008; Smirnov and Pedersen, 2009; Wilde-Piorko et al., 2010).

Within both Phanerozoic and Precambrian Europe there are significant lateral variations in the depth to the LAB, particularly associated with Alpine subduction. In general, the variations in Precambrian Europe are smoother, except for the western and northern boundaries towards the oceans and the southern boundary towards the TESZ.

As we will show, our estimators of the depths to the LAB are nowhere all three consistent with one another — in Phanerozoic Europe two of them agree with each another, to within statistical error, whereas in Precambrian Europe a different two of them agree. From these similarities and differences lies information about the

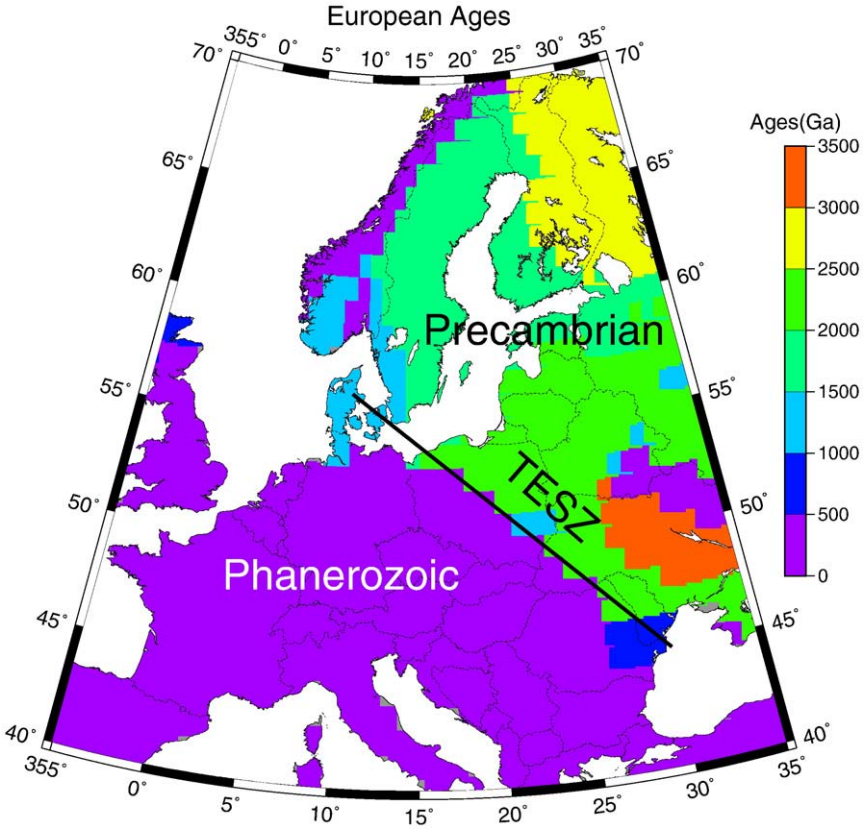

Fig. 1. Age domain map of Europe (from I. Artemieva, 2008, pers. comm.).

nature of the LAB, with the strong inference that it is not the same at all places.

2. Estimates of the depth to the LAB in Europe

2.1. Seismic anisotropy LAB — sLABa

Plomerova, Babuska and colleagues (Babuska and Plomerova, 1992; Plomerova et al., 2002b) define the LAB as the depth at which seismic anisotropy direction changes from a lithospheric "fossil" direction to an asthenospheric plate-flow direction parallel to APM. Herein we term these the "sLABa" estimates. Changes in orientation of anisotropy intensify the P-velocity contrast above and below the LAB, and are reflected in radial and azimuthal anisotropy of surface waves. A full description of the analysis approach and the results obtained for Europe is given in a companion paper in this volume (Plomerova and Babuska, 2010), to which the interested reader is referred. For completeness, below we give a short description of the Strengths and Weaknesses of all methods.

2.1.1. Strengths

The strength of this single station method, based on an empirical relation between relative P-wave travel time delays (residuals) and the LAB depths, is in its sensitivity to lateral changes of lithospheric thickness, which is independent of region parameterization. The accuracy of the mean representative residuals is usually better than ± 0.1 s, which allows us to estimate the sLABa depth variations with an accuracy of ~ ± 10 km. Considering steep rays used to calculate static terms of the relative residuals, the station means represent volumes with radii of about 25, 40 and 60 km at depths 50, 100 and 150 km, respectively. No *a priori* velocity–depth distribution in the upper mantle is required (Babuska and Plomerova, 1992).

2.1.2. Weaknesses

The sLABa estimates require good knowledge of the structure of the crust—P-velocity and Moho depth, and especially thickness and velocity of a sedimentary cover if present beneath a station. Only after applying proper time corrections for crustal effects can the variations of the P residuals be associated with variations of the sLABa depths. A limitation can come from considering the "LAB depth-P-residual" relation constant at provinces of different ages with potentially different inclinations of lithospheric mantle fabrics (Babuska et al., 1998).

2.1.3. Results for Europe

This seismic anisotropy LAB, sLABa, was mapped across Europe using the data from a variety of seismic experiments (Plomerova et al., 2002a; Babuska and Plomerova, 2006; Plomerova et al., 2006, 2008; Plomerova and Babuska, 2010). The sLABa estimates for Europe are shown in Fig. 2, and in histogram form in Fig. 8. The minimum and maximum values are 32 km (beneath the Danish Basin) and 250 km (northwestern Alps), with the mean of the 657 estimates being

$$sLABa = 137 \pm 48\text{km}.$$

(Note: all statistical estimates of various subsets are shown in Table 1.)

We can obtain robust estimates of the mean and range by using outlier rejection. Rejecting the 10 points that lie outside the 95% confidence limits of 42–232 km yields a mean and range of

$$sLABa = 138 \pm 46\text{km}.$$

However, a statistical test for unimodality, namely '*diptst1*' of Hartigan (1985) based on Hartigan and Hartigan (1985) with F. Mechler and Y. Lu's corrections, yields a dip statistic of 0.034, inferring that there

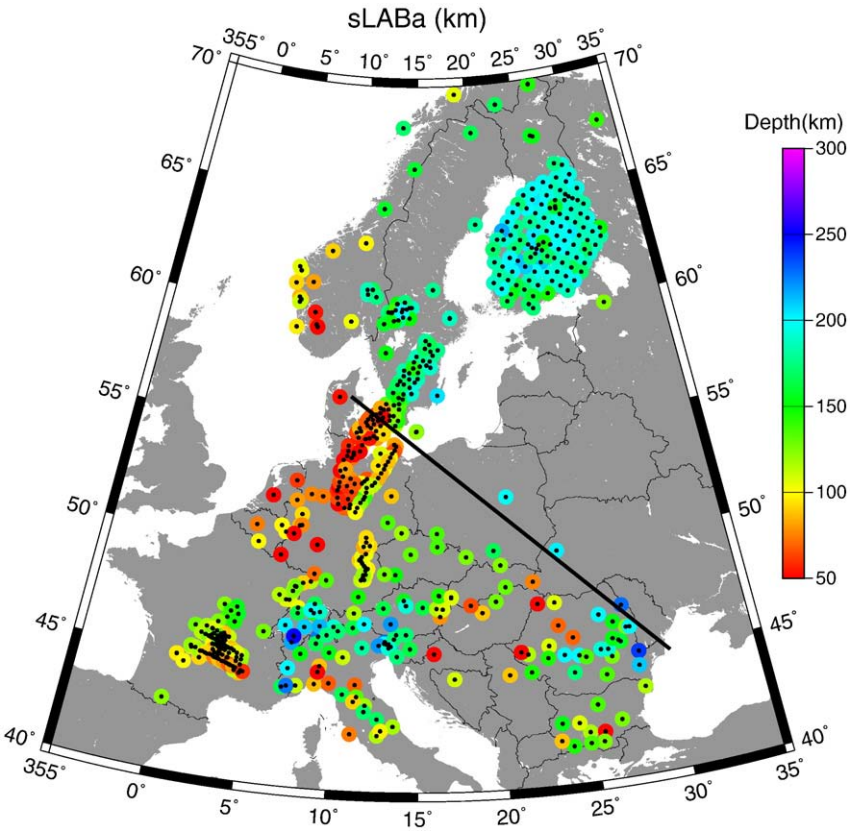

Fig. 2. Estimates of the depth to the seismic anisotropically defined LAB, the sLABa, from Plomerova et al. (2002a), Babuska and Plomerova (2006), Plomerova et al. (2006), Plomerova et al. (2008) and Plomerova and Babuska (2010).

Table 1
Statistical estimates of the depth to the lithosphere–asthenosphere boundary from the different techniques and subsets.

	sLABa [km]	sLABrf [km]	eLAB [km]
All	137 ± 48	106 ± 34	170 ± 112
Within 95% of mean	138 ± 46	96 ± 18	153 ± 95
LABs < 150 km	100 ± 27		78 ± 28
LABs > 150 km	183 ± 19		250 ± 51
Phanerozoic[a]	118 ± 45	96 ± 17	98 ± 56
–Median smoothed[b]	133 ± 49		89 ± 49
Precambrian	169 ± 35	172 ± 26	237 ± 66
–Median smoothed	182 ± 13		253 ± 29

[a] Alps excluded.
[b] Northern Germany excluded.

is more than one peak in the depth distribution, as is visually evident in Fig. 8. The sLABa estimates have two peaks, one at around 80–100 km and the other at around 180–200 km, so the mean sLABa of all values is meaningless as it actually lies within the minimum between these two peaks. Splitting the sLABa depth estimates into two groups, <150 km and >150 km, the means of the two groups are

$$sLABa_{<150} = 100 \pm 27\text{km, and } sLABa_{>150} = 183 \pm 19\text{km}$$

with the shallower depths (red circles, Fig. 10) representative of predominantly Phanerozoic Europe and the deeper depths (blue circles, Fig. 10) of Precambrian Europe and the Alpine region. Note that, as would be expected, splitting the sLABa depths into shallow and deep groups significantly reduced deviations (variance) of the averages—from 46 km for the combined average to 27 and 19 km, respectively. For Phanerozoic Europe, excluding the Alps, and for Precambrian Europe, the averages and ranges are

$$sLABa_{\text{Phan}} = 118 \pm 45\text{km, and } sLABa_{\text{Precam}} = 169 \pm 35\text{km.}$$

To avoid issues related to data sampling biases, the sLABa estimates were smoothed using the Generic Mapping Tools (GMT) function *blockmedian* with a width of 2 degrees and a tension of 0.5. The 108 estimates are shown in Fig. 3, and in histogram form in Fig. 9. Fig. 3 more strikingly displays the shallow sLABa beneath the Danish and North German Sedimentary Basins, the shallower sLABa on the Norwegian coast, and the deep sLABa beneath the central part of the Baltic Shield in Finland. The smoothing minimizes the extent of the Pannonian Basin as a result of the fact that the basin is surrounded by the deep lithosphere beneath the Carpathians and the Eastern Alps. If the shallow values for the Danish and North German Sedimentary Basins are excluded, then the averages for Phanerozoic and Precambrian Europe become

Phanerozoic Europe

$$\text{sLABam} = 133 \pm 49\text{km,}$$

Precambrian Europe

$$sLABam = 182 \pm 13\text{ km.}$$

The TESZ is visible in both single value and smoothed sLABa depth images (Figs. 2 and 3) with a strong change in the depth to the LAB. This step-like change of ~100 km is greater than the difference between the two mean values between Phanerozoic and Precambrian Europe.

2.2. Seismic S-wave receiver function LAB — sLABrf

The S-to-P receiver function (SRF) technique is a relatively new technique that is capable of identifying especially the LAB over the more conventional P-to-S RF method (PRF) (Yuan et al., 2006). The PRF method is not as sensitive to the LAB given the velocity inversion

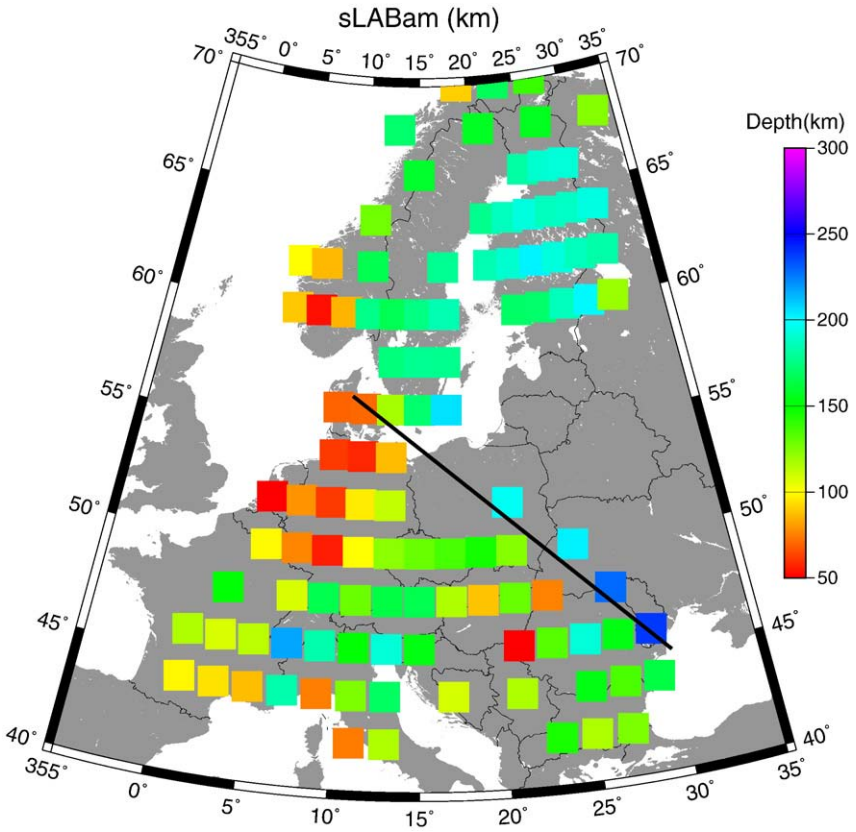

Fig. 3. Median smoothed sLABa estimates, sLABam, of Fig. 2. Smoothing by median filtering using the Generic Mapping Tools (GMT) function *blockmedian* with a width of 2 degrees and a tension of 0.5.

that occurs with slower velocities in the upper asthenosphere and faster velocities in the lower lithosphere. The SRF technique has been used in many tectonic settings (Kumar et al., 2005; Sodoudi et al., 2006a, b; Heit et al., 2007; Sodoudi et al., 2009) and results have recently been produced for Europe (Geissler et al., 2010), to which the interested reader should refer for more detailed description. Rychert et al. (2010) provide a recent global compilation of both PRF and SRF results and a discussion of the strengths and weaknesses of the RF method. The results for Europe from Geissler et al. (2010) are analysed here, and are termed the "sLABrf" estimates.

2.2.1. Strengths

The most significant strength of this technique is that SRFs are very sensitive to rapid impedance contrasts, and can therefore infer important information about the abruptness of the LAB. SRF modelling shows that generally the LAB is relatively sharp with an overall sharpness of less than 20 km (Li et al., 2007; Kawakatsu et al., 2009; Rychert and Shearer, 2009). Moreover, the SRFs are not biased by crustal multiple conversions as are P-to-S receiver functions (PRFs). The S receiver function technique is successful in observing the LAB with high resolution and density and has the potential to gain the same significance for the lower lithosphere as steep angle seismics for the upper lithosphere.

2.2.2. Weaknesses

One general weakness of RFs is that they require an accurate velocity model to convert from time to depth, which is provided through other seismological techniques. Taking into consideration the maximum depth resolution of the SRF as well as possible bias error due to the reference model used, an error of ± 10 km must be considered in sLABrf depth estimates.

The presence of thick sedimentary layers must be considered in estimating the LAB depth. However, regarding the error (~10 km) introduced in the sLABrf depth estimation, and due to the lack of reliable local velocity models, this effect has been neglected in the study of Geissler et al. (2010).

2.2.3. Results for Europe

The sLABrf estimates derived by Geissler et al. (2010) at 47 locations in predominantly central Europe are shown in Fig. 4. The mean of the sLABrf estimates is

$$sLABrf = 106 \pm 34\text{km}.$$

Rejecting the 5 points that lie outside the 95% confidence limits of 37–174 km yields a mean of

$$sLABrf = 96 \pm 18\text{km}.$$

The rejected values are those that lie to the northeast, i.e., north of the TESZ. Thus, this robust average sLABrf estimate is valid for central Phanerozoic Europe.

The median-smoothed sLABrf estimates (sLABrfm) are shown in Fig. 5, and the variation across the TESZ is clearly marked in these estimates. The averages and standard deviations on either side of the TSZ are:

Phanerozoic Europe

$$sLABrfm = 96 \pm 17\text{km}(26\text{values}),$$

Precambrian Europe

$$sLABrfm = 172 \pm 26\text{km}(5\text{values}).$$

In terms of the nature of the LAB, Geissler et al. (2010) found a sharp LAB beneath the Phanerozoic platform of Central Europe, but

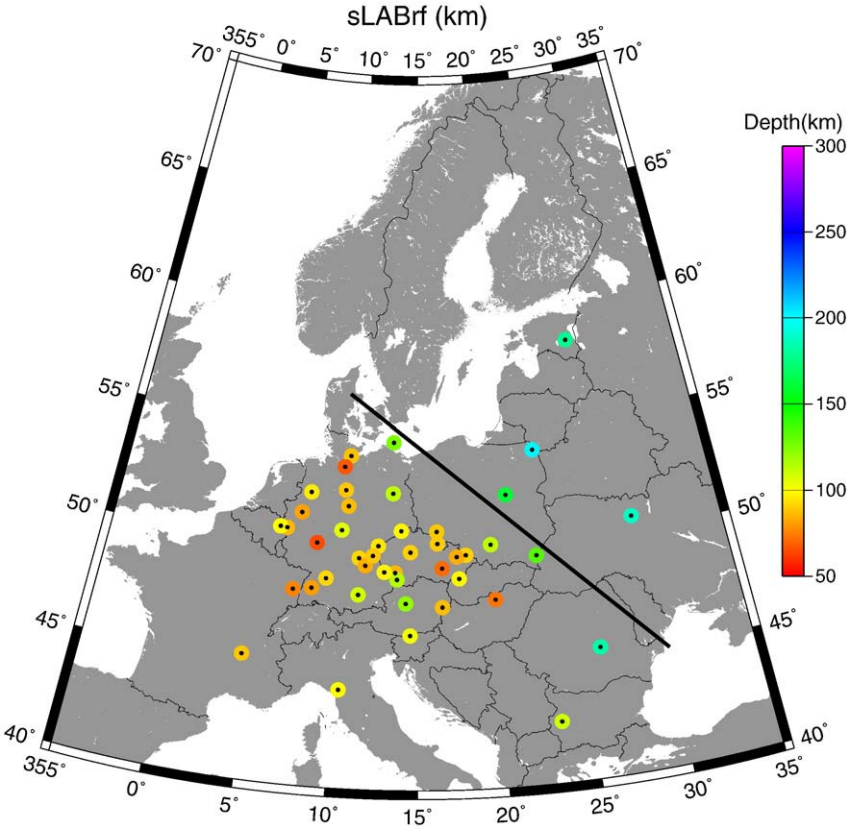

Fig. 4. Estimates of the depth to the S-to-P defined LAB, the sLABrf, from Geissler et al. (2010).

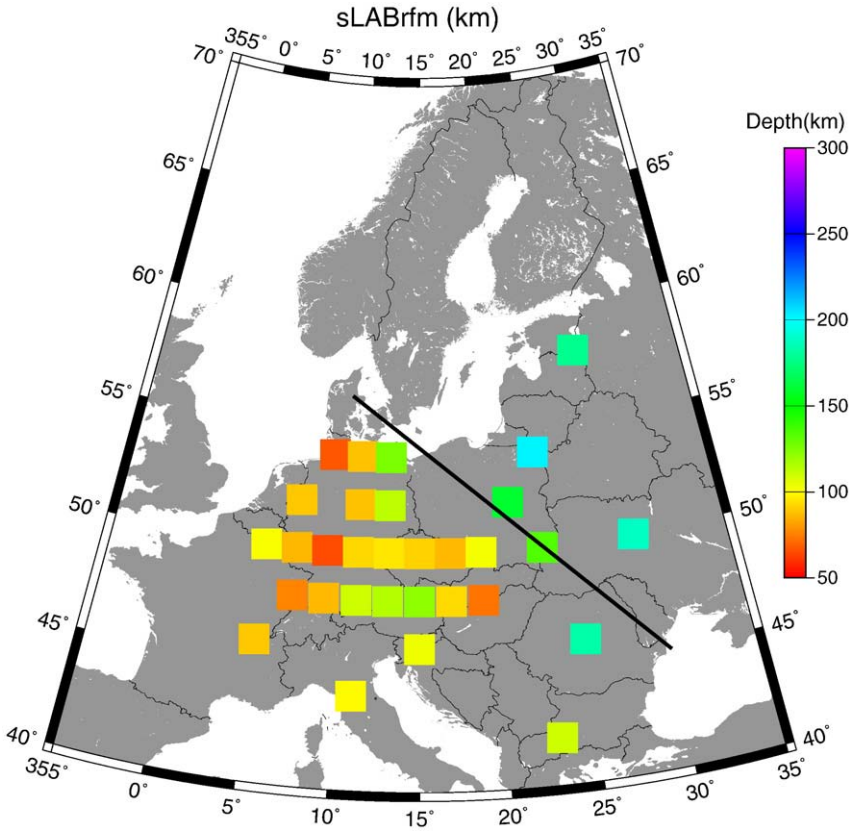

Fig. 5. Median smoothed sLABrf estimates, sLABrfm. See caption to Fig. 3 for details.

the converted phase from the LAB beneath the Precambrian platform of Eastern Europe is not as sharp as that found beneath other stations located in Central Europe.

2.3. Electrical LAB — eLAB

The electrical LAB (eLAB) is traditionally identified by a rapid reduction in electrical resistivity, i.e., rapid increase in electrical conductivity, at upper mantle depths (Heinson, 1999; Jones, 1999). Mantle minerals in the lithosphere will be resistive (Ledo and Jones, 2005; Jones et al., 2009), unless there exists some unusual and exotic conducting phases, such as graphite or sulphides (Jones, 1999). The asthenosphere has low resistivity, with global compilations suggesting values in the range 5–25 Ω m (Heinson, 1999). Driven principally by thinking about the nature of oceanic asthenosphere, explanations for the low resistivity beneath continents have traditionally been in terms of an interconnected network of partial melt with very low melt fraction (1–5%) — any higher would be gravitationally unstable (Ghods and Arkani-Hamed, 2000; Tirone et al., 2009).

Almost two decades ago an alternative explanation was proffered, namely hydrogen diffusion in "wet" rocks (Karato, 1990). Some have appealed to this explanation in preference to partial melt (Hirth et al., 2000; Evans et al., 2005), but in his excellent review on sensing hydrogen in the mantle, Karato (2006) points out that the experimental data do not really exist to support some of his 1990 assumptions. However, the point of this paper is not to debate the topic of why there is an electrical asthenosphere, but to show its correlation, or otherwise, with other estimates of the LAB depth. Korja's (2007) compilation of the depth to the electrical LAB are used here, and are termed the "eLAB" estimates.

2.3.1. Strengths

The greatest strength of electromagnetic methods is that the parameter EM methods are responsive to at low frequency, namely electrical conductivity, varies by many orders of magnitude, and in particular, has high sensitivity to the onset of an interconnected conducting phase increasing by 1–2 orders of magnitude when melting initiates (Partzsch et al., 2000; Maumus et al., 2005). Particularly the transition from the lithosphere to the asthenosphere, whether it is due to wet conditions (Karato, 1990, 2006) or partial melt or both, will increase conductivity by orders of magnitude. Of available EM methods, the natural-source magnetotelluric technique is preferred as it penetrates to all depths, but with decreasing resolution. The alternative is very large-scale controlled source EM experiments, such as the Khibiny MHD generator on the Kola Peninsula (Velikhov et al., 1986), but these are impractical for field campaigns.

Sensitivity tests indicate that with modern, high quality MT data (errors <2% in impedance) the onset of the asthenosphere can be sensed to a precision of 10% or better (Jones, 1999).

2.3.2. Weaknesses

The magnetotelluric method has undergone significant improvement since its theoretical inception in the early-1950 s. Particularly since the early-1990 s there have been major advances in almost all aspects, from instrumentation to processing to analysis to modelling to inversion. Accordingly, one needs to be very careful that the most modern and advanced methods have been applied to the data, and older results, or results obtained that do not use modern methods, may not be reliable.

The Earth response function derived from the observations, the MT impedance tensor, is in almost all cases interpreted as resulting from a

uniform source field. Major effort is expended by MT specialists when dealing with time series that may be contaminated by non-uniform source field structure (Jones and Spratt, 2002; Varentsov et al., 2003). Generally, the effects will lead to an *underestimate* in the depth to the LAB (see Jones and Spratt, 2002), although that is not always the case (Jones, 1980).

In addition, some of the eLAB estimates comes from single site 1D inversions (see Korja, 2007 for details) so may suffer from the effects of *static shifts* (see, e.g., Jones, 1988). However, the compilation relied on the results from more sophisticated 2D models where available.

2.3.3. Results for Europe

Recently, Korja (2007) assessed estimates of eLAB depths provided by interpretations of primarily magnetotelluric data from a wide range of experiments held across Europe, and critically selected those in which he had confidence. The 245 eLAB estimates for Europe in Korja's database are shown in Fig. 6, and block averaged in Fig. 7. The minimum and maximum values are 20 km (Apennines) and 410 km (N of TESZ). These LAB estimates clearly have the largest range of the three estimators, and the mean, with its significantly large standard deviation, is

$$eLAB = 170 \pm 112\text{km}.$$

Rejecting the 17 points that lie outside the 95% confidence limits of 0–394 km, i.e., all of those with default values of 400 km or 410 km, yields a mean of

$$eLAB = 153 \pm 95\text{km}.$$

The statistical test for unimodality yields a dip statistic of 0.041 confirming what is visually obvious in Figs. 6, 8 and 9 that there is more than one peak in the eLAB depth distribution, with one strong shallow peak at 60–80 km and a broader deeper peak centred on 240–260 km. Thus, as with the sLABa, the mean is meaningless and lies between two peaks in the distribution. Splitting the eLAB depth estimates into two groups, <150 km and 150–350 km, the means of the two groups are

$$eLAB_{<150} = 78 \pm 28\text{km}, \text{and } eLAB_{150-350} = 250 \pm 51\text{km}$$

with the shallower depths (green squares, Fig. 10) representative of Phanerozoic Europe and the deeper depths (purple squares, Fig. 10) of predominantly Precambrian Europe. Splitting the database into two groups by age of crustal rocks, as shown in Fig. 1, excluding the Alps and the ultra-deep values north of the TESZ, yields the means and spreads for Phanerozoic and Precambrian Europe

$$eLAB_{\text{Phan}} = 98 \pm 56\text{km}, \text{and } eLAB_{\text{Precam}} = 237 \pm 66\text{km}.$$

The anomalously deep values of the depth to the first mantle conductor of around 350–400 km just north of the TESZ is best seen in the very careful work of Smirnov and Pedersen (2009), who studied the Sorgenfrei–Tornquist Zone branch of the TESZ in southern Sweden and Denmark. Such resistive mantle to effectively the transition zone is very surprising, and these cannot be considered depths to the "LABs"—essentially there is no evidence of an electrical asthenosphere beneath and directly to the north of the TESZ. On their own, one might be tempted to discount these deep depths as due to inappropriate analysis and modelling, and invoke effects such as source field contamination, although non-uniform source fields will generally bias LAB estimates to shallower levels (e.g., Jones and Spratt, 2002). However, a recent analysis of annual means from European magnetic observatory data by Dobrica and Demetrescu (2009) for very long period/deeply-penetrating information showed a NW–SE strip of high resistivity/high inductance through Europe that is spatially coincident with the location of the TESZ. Such high resistivities imaged by

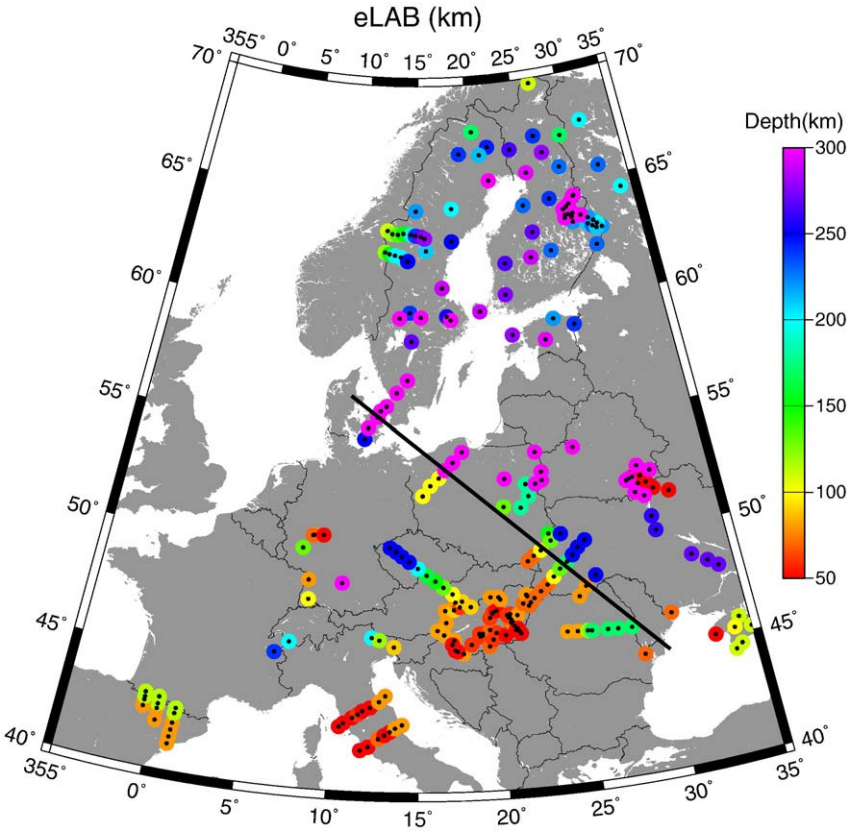

Fig. 6. Estimates of the depth to the electrically-defined LAB, the eLAB, from Korja (2007).

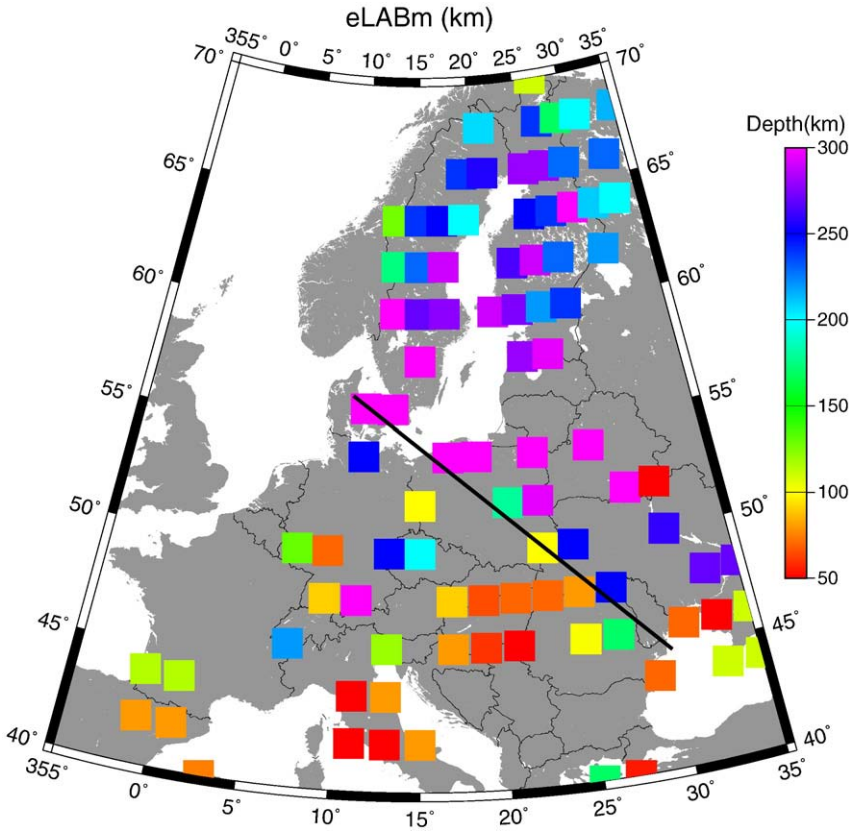

Fig. 7. Median smoothed eLAB estimates, eLABm. See caption to Fig. 3 for details.

Smirnov and Pedersen (2009), of 300 Ω m at 300–350 km depths, are consistent with laboratory determinations of dry mantle minerals (for review of the literature, see Jones et al., 2009). Using the simple pure olivine SEO3 model of Constable (2006), for a temperature of 1350–1400 °C, one would expect a resistivity of 350–250 Ω m, which is what is observed by Smirnov and Pedersen (2009). Thus, on the basis of the EM results we can exclude any suggestion of partial melt or hydration of the upper mantle in this region.

2.4. Seismic tomography

Regional-scale seismic body wave tomography gives excellent information about lateral variations, but is less sensitive to sharp changes in velocity, and the LAB in particular, than the other seismological techniques. However, the results can be usefully used in a qualitative sense comparing seismic velocities at a given depth.

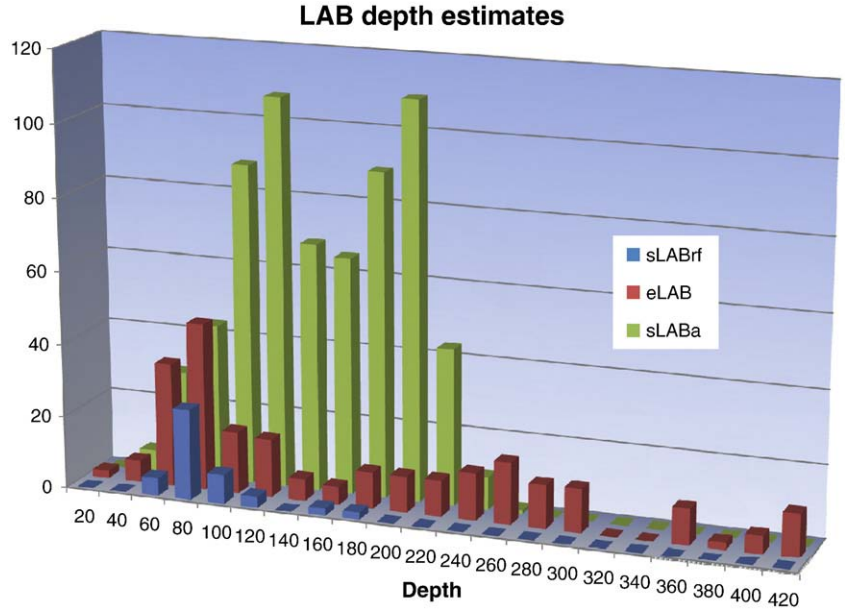

Fig. 8. Histograms of all three LAB estimates of Figs. 2, 4 and 6. sLABa in green at the back, eLAB in red in the middle, and sLABrf in blue in the front.

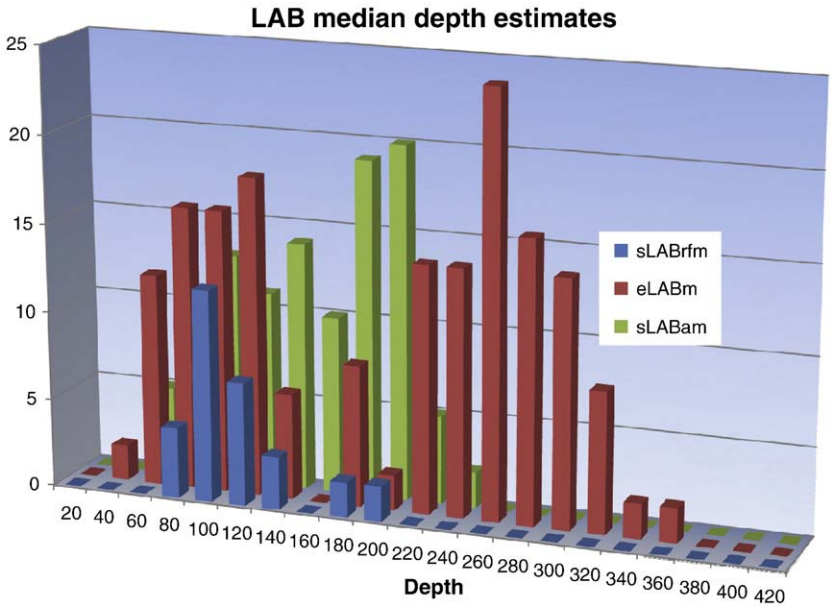

Fig. 9. Histograms of all three median smoothed LAB estimates of Figs. 3, 5 and 7. sLABam in green at the back, eLABm in red in the middle, and sLABrfm in blue in the front.

2.4.1. Strengths

The greatest strength of body wave tomography is its ability to sense both lateral and vertical variations in seismic velocity, albeit with differing resolution.

2.4.2. Weaknesses

One weakness of body wave topographic methods is the prevalence for vertical smearing of structures along arrival paths, especially in regions of poor ray coverage. Also length-scale of mapping of lateral variations is restricted to horizontal parameterisation of the velocity model (size of blocks or node spacing).

2.4.3. Results for Europe

Fig. 11 displays a slice at 260 km depth from the new body wave tomographic model of Europe from Spakman (unpubl.) using the travel time information for Europe of Amaru et al. (2008). The original

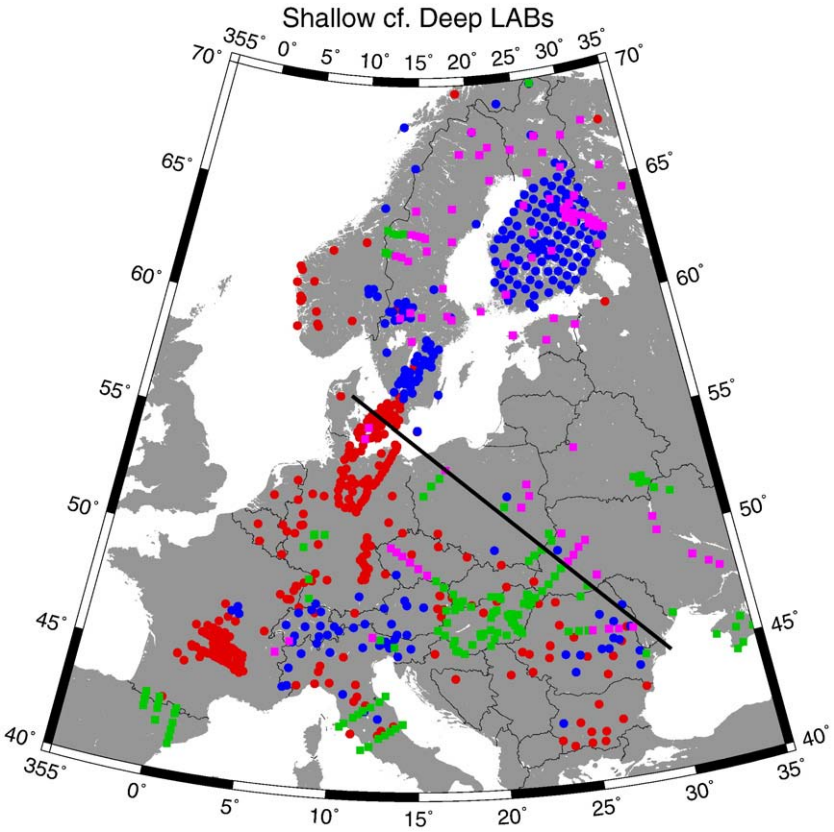

Fig. 10. Shallow (<150 km) and deep (>150 km) LAB estimates. Shallow sLABa estimates are dots in red, and deep sLABa estimates in blue. Shallow eLAB estimates are squares in green, and deep eLAB estimates are in purple.

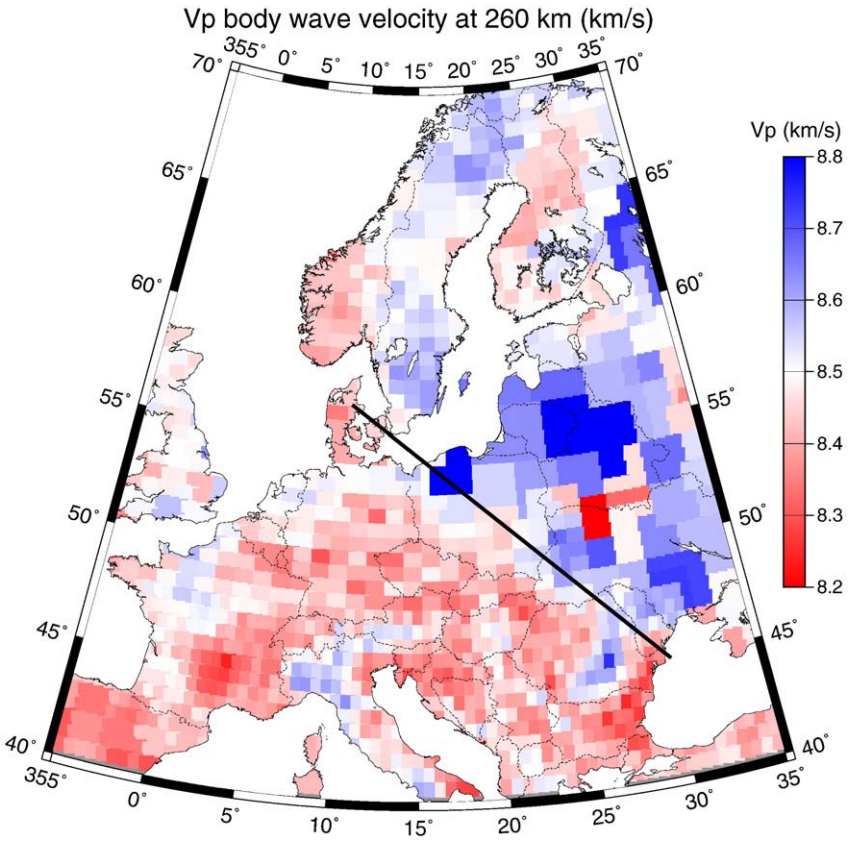

Fig. 11. Seismic Vp absolute velocity at 260 km depth from Spakman (unpubl.). Original velocity anomaly map in percent was converted to velocity using a value of 8.48 km/s, which is the Vp velocity at 250 km from ak135.

model velocity data were in percentage differences from a standard model, namely ak135 (Kennett et al., 1995). The data have been adjusted relative to a velocity of 8.48 km/s, the velocity at 260 km in ak135, and plotted as absolute velocity in Fig. 11. This depth was chosen as to be below most estimates of the LAB. The TESZ is clearly visible at 260 km separating a southern region of velocity below 8.5 km/s from a northern region with velocity above 8.5 km/s.

3. Quantitative statistical comparisons of LAB estimates

3.1. sLABrf cf. sLABa

Fig. 12 shows a cross-plot between 35 sLABrf and sLABa depth estimates, for observation locations that are within 25 km of each other. If both estimators are unbiased, they would scatter around the 1:1 solid black line, whereas clearly the majority of points lie above the 1:1 line inferring that sLABa estimates are systematically larger than sLABrf estimates. A linear regression analysis, assuming both sets of data are in error (York, 1966; 1969; Fasano and Vio, 1988), of the 35 points yields

$$sLABa = -84.1(\pm 1.7) + 2.08(\pm 0.02) * sLABrf\,(\mathrm{km}),$$

(dotted black line) with a correlation coefficient of only 0.59. Using robust statistics to identify and reject outliers (Huber, 1981), the two statistical "outlier" values at large sLABrf/sLABa are downweighted and a robust York-Fasano linear regression gives

$$sLABa = -108.5(\pm 2.3) + 2.38(\pm 0.02) * sLABrf\,(\mathrm{km}),$$

(dashed black line) with a correlation coefficient of 0.86.

A more useful examination of the two datasets is to inspect a geographic plot of the difference between the two, i.e., sLABrf–sLABa, for systematic variation. Fig. 13 shows that there is a consistent geographic distribution of the differences. All of the estimates where

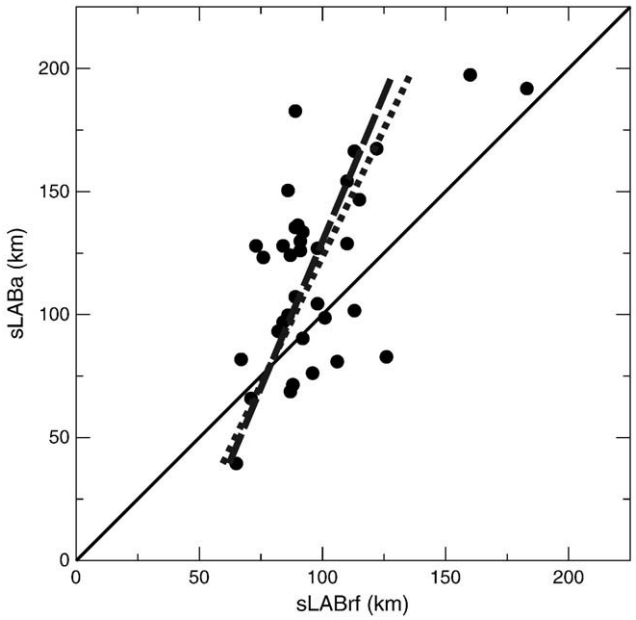

Fig. 12. Cross-plot of raw sLABrf estimates against raw sLABa estimates for locations that are within 25 km of each other. The solid black line is the 1:1 line that the data should scatter around if there are no bias errors. The dotted line is a linear regression analysis, assuming both sets of data are in error. The dashed line is a robust linear regression with outlier rejection.

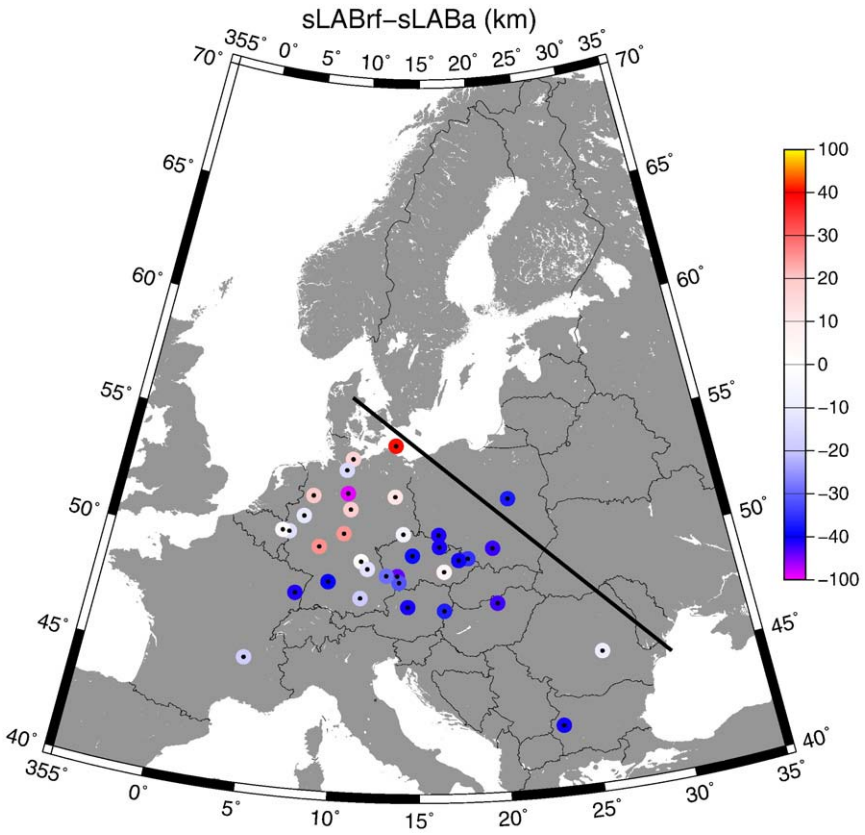

Fig. 13. The difference between the sLABrf and the sLABa estimates (in km) for locations that are within 25 km of each other.

sLABrf>sLABa are located in northern Germany north of latitude 50°N, predominantly on the North German sedimentary basin, whereas the majority of the estimates, for which sLABrf<sLABa, are located across the rest of Europe. There is a highly anomalous point in northern Germany for which the sLABrf–sLABa difference is largest at −93.7 km (purple point in Fig. 9), and a second close to the TESZ for which the difference is largest positive at +43.2 (red point at TESZ in Fig. 9).

The LAB averages for the 11 points in Germany north of latitude 50°N, excluding the two anomalous ones referred to above, are sLABrf = 90 ± 15 km and sLABa = 83 ± 19 km, with an averaged (sLABrf–sLABa) difference of +7 ± 16 km. An F-test for the two depth sets yields an F-ratio of 0.15 indicating that the two datasets are statistically indistinguishable. A robust York-Fasano linear regression of these 11 points gives:

$$sLABa = -63.8 + 1.62 * sLABrf\,(\mathrm{km})$$

with a correlation coefficient of 0.73.

The LAB averages for the remaining 23 points in south-central Europe are sLABrf = 99 ± 27 km and sLABa = 132 ± 32 km, for an average difference of −33 ± 18 km. A robust York-Fasano linear regression of these 23 points gives:

$$sLABa = 6.6 + 1.28 * sLABrf\,(\mathrm{km})$$

with a high correlation coefficient of 0.87, which is close to the desired result of 1:1 with zero intercept.

The F-ratio between these two sets of differences, i.e., (sLABrf–sLABa) for the set of 11 points in Germany north of latitude 50°N and the set of 23 other points, is 5.12, which is significantly above the upper critical 5% $F_{0.05}(1,32)$ value of 4.15, so we can confidently reject the null hypothesis that these two sets are statistically the same. Thus, the LAB we are sensing with receiver functions and with anisotropy directions, the two methods used herein, operate differently where there is thick sedimentary cover compared to where there is none. Where there is cover the two methods yield the same result, to within error. Where there is no sedimentary cover, the sLABrf is shallower than the sLABa by 33 ± 18 km on average.

3.2. eLAB cf. sLABa

Fig. 10 shows a qualitative comparison of the regions of shallow (red and green in Fig. 10) and deep (blue and purple in Fig. 10) seismic anisotropy (sLABa) and electrically-defined (eLAB) LAB. Generally the estimates are qualitatively consistent, such as central Scandinavia (deep), Alps (deep), Pannonian Basin (shallow), Germany (shallow), Italy (shallow), and particularly the shallow-to-deep transition crossing the TESZ from southwest to northeast.

However, there are some regions for which the two are not in agreement, such as the Danish Basin and the Bohemian Massif (Czech Republic), though for the latter an earlier comparison study between MT and LABa results (Praus et al., 1990) did find good correlation. Such discrepancies for localised regions require further work.

Fig. 14 shows a cross-plot between eLAB and sLABa estimates, for observation locations that are within a distance equal to the eLAB depth of each other. At first glance, ignoring the colour coding, the cross-plot suggests that there is indeed no strong correspondence between the two LAB estimates as the points appear to scatter around the 1:1 line (black line). However, the differences between the two, i.e., (eLAB–sLABa), when plotted geographically (Fig. 15) display a consistent grouping, with eLAB>sLABa at almost all locations in Precambrian Europe north of the TESZ, and eLAB<sLABa at most locations in Phanerozoic Europe south of it (Fig. 15), with the already marked notable exception of sites in the Bohemian Massif (Czech Republic).

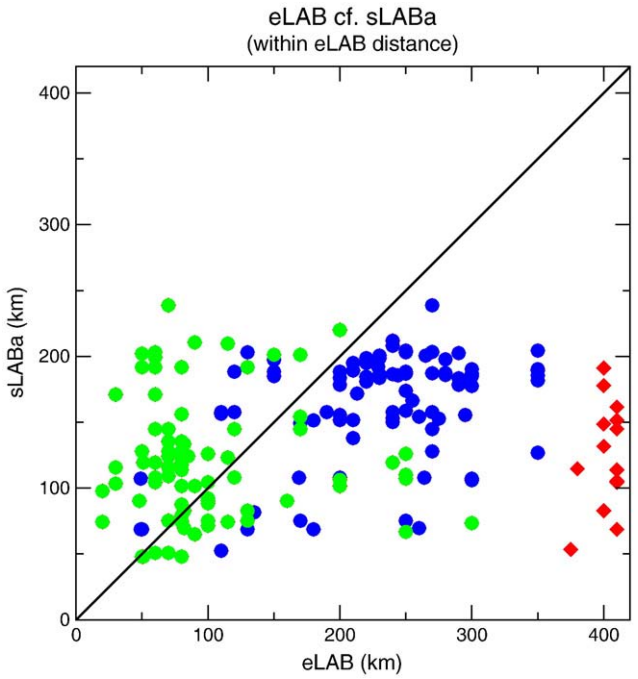

Fig. 14. Cross-plot of raw eLAB against raw sLABa estimates for stations within an eLAB depth of each other. Green points are those from Phanerozoic Europe, blue points are from Precambrian Europe, and the red points are from the locations where the eLAB estimates are ultra-deep just to the north of the TESZ. The solid black line is the 1:1 line that the data should scatter around if there are no bias errors.

Applying the same statistical procedures as in the previous section for the two distinct groupings, i.e., Precambrian and Phanerozoic Europe, we obtain the following (excluding the highly anomalous red points):

Precambrian Europe: 101 points (blue points on Fig. 14)

$$eLAB = 237 \pm 66\text{km}, sLABa = 169 \pm 35\text{km},$$
$$eLAB - sLABa = +66 \pm 65\text{km}.$$

Phanerozoic Europe (excluding Alps): 104 points (green points on Fig. 14)

$$eLAB = 98 \pm 56\text{km}, sLABa = 118 \pm 45\text{km},$$
$$eLAB - sLABa = -20 \pm 72\text{km}$$

Fig. 16 shows histograms of the two sets of differences. Clearly for Precambrian Europe there are few locations where eLAB<sLABa and there is a single peak to the histogram, but with a long tail. For Phanerozoic Europe most of the differences are such that eLAB<sLABa, but the histogram is bi-modal with a peak at around −40 km and another at +20 km. The positive peak is associated with locations predominantly in the Bohemian Massif (Czech Republic).

Repeating the above but for the median-smoothed data, to remove sampling biases, we obtain the difference plot shown in Fig. 17. The average means are

Precambrian Europe: 20 points (Scandinavian locations on Fig. 17)

$$eLABm = 253 \pm 29\text{km}, sLABam = 182 \pm 13\text{km}, eLABm - sLABam = +76 \pm 36\text{km}.$$

The F-ratio between these two depth sets is 7.97, which is far higher than the 5% critical $F_{0.05}(1,38)$ value of 4.10 and even exceeds the 1% critical $F_{0.01}(1,38)$ value of 7.50, so we can be very confident in our assertion that the eLAB and sLABa are not sensing the same interface in Precambrian Europe.

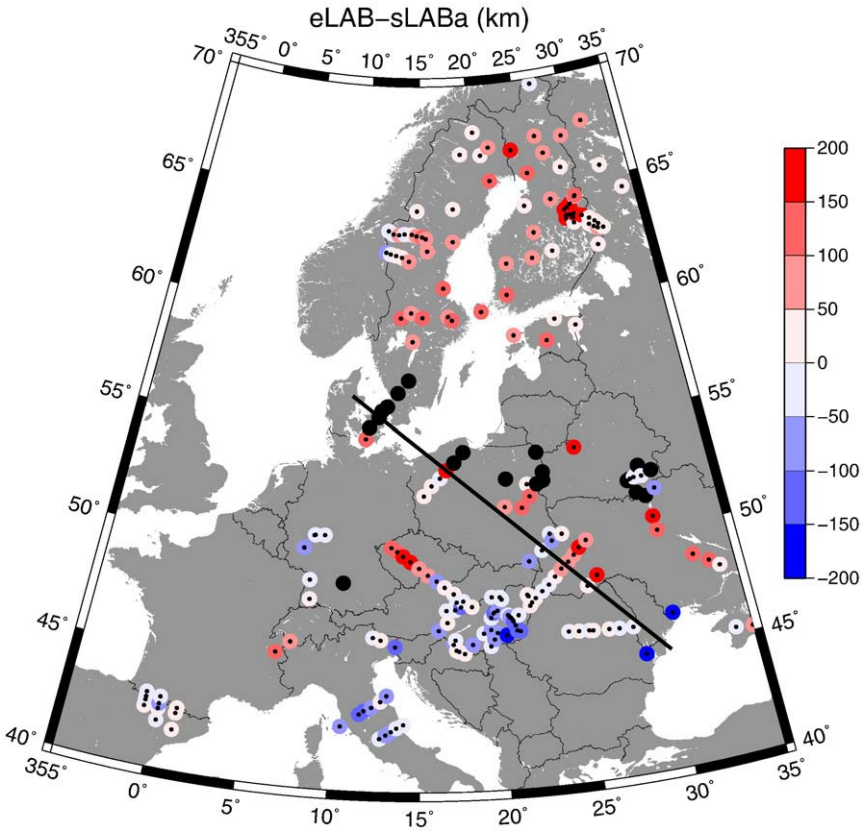

Fig. 15. The difference between the eLAB and the sLABa estimates at eLAB locations within eLAB depth distance of an sLABa location. Black dots are differences >200 km.

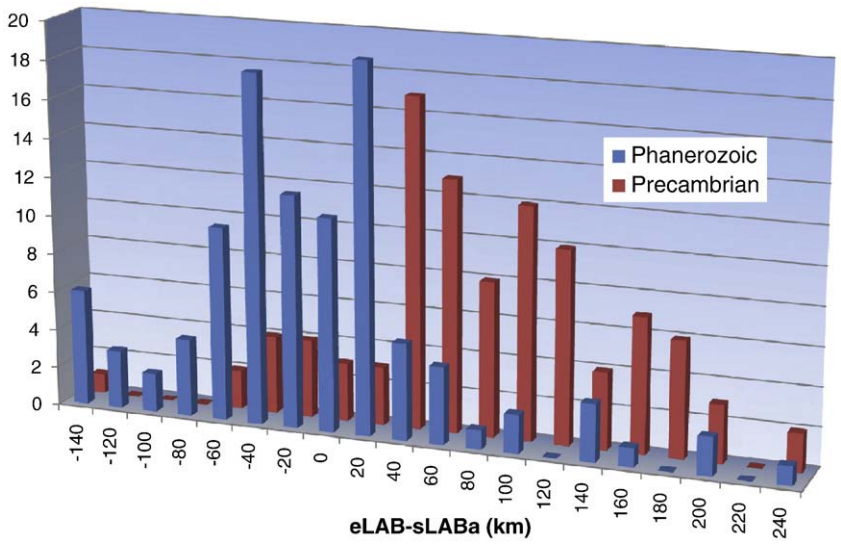

Fig. 16. Histogram of the differences between eLAB and sLABa estimates for Precambrian (red bars) and Phanerozoic (blue bars) Europe.

Phanerozoic Europe (north of 50°): 5 points (northern Europe locations west of the TESZ on Fig. 17)

$eLABm = 180 \pm 79$km, $sLABm = 88 \pm 36$km, $eLABm-sLABam = +92 \pm 69$km.

Phanerozoic Europe (excluding northern Germany): 16 points (central and southern Europe locations west of the TESZ on Fig. 17)

$eLABm = 89 \pm 49$km, $sLABam = 133 \pm 49$km, $eLABm-sLABam = -43 \pm 41$km.

Whilst the four sets of depths for Phanerozoic Europe above (eLABm and sLABam) cannot be statistically separated, an F-test statistic on the two sets differences of (eLABm–sLABam) gives an F-ratio of 7.86, which is significantly above the $F_{0.05}(1,19)$ value of 4.38 and even is close to the 1% critical $F_{0.01}(1,38)$ value of 8.19. Thus we can be confident in our assertion that there is a significant difference between northern Europe and central and southern Europe in our sensing of the LAB using the two different techniques.

4. Discussion

The statistical examination of the sLABrf and sLABa datasets demonstrates that the two can be separated into two subsets, one of 11 locations in Germany north of latitude 50°N and the other 23 locations in central Europe (Fig. 13). For the former the sLABrf is deeper than the sLABa by 7 km on average, so are the same to within experimental scatter and error, whereas for the latter the sLABrf is shallower than the sLABa by 33 km on average. The two sets of differences, i.e., (sLABrf–sLABa), for (1) the German 11 points and (2) the other 23 points fail the F-test hypothesis that they come from the same distribution, so statistically one can be confident in concluding that they are different. It is interesting to note that the two are in close agreement in an area of thick sedimentary cover (North German Sedimentary Basin), but not in agreement where such cover is absent. The differences between how sedimentary cover is treated by the two methods may explain some of the discrepancy, but certainly not a difference of 33 km.

The statistical examination of the eLAB and sLABa datasets shows that there is a significant systematic differences between the two, with eLAB>sLABa for Precambrian Europe, by approx. 76 km, and eLAB<sLABa for Phanerozoic Europe by approx. 43 km (Fig. 15). Both of these are a puzzle. For Scandinavia, whatever is causing the seismic anisotropy at an average depth of around 170 km is not seen in the magnetotelluric data with its average depth of 240 km. For northern Karelia/southern Lapland, there does appear to be reasonable correlation, with a 1D model from one site (B42) indicating a rapid increase in electrical conductivity at a depth of around 170 km (Lahti et al., 2005), consistent with the sLABa value. This one location is anomalous though in such a correlation, as otherwise the eLAB is systematically greater than the sLABa estimates (compare Figs. 2 and 6).

Removing sampling biases by considering the median smoothed LABs for Phanerozoic Europe and Precambrian Europe, we find that the means and spreads of the estimates of the LAB are:

Phanerozoic Europe

$eLABm = 89 \pm 49$km, $sLABam = 133 \pm 49$km, $sLABrfm = 96 \pm 17$km,

and

Precambrian Europe

$eLABm = 253 \pm 29$km, $sLABam = 182 \pm 13$km, $sLABrfm = 172 \pm 26$km.

These averages can be compared to the recent global compilation of depths to the LAB from studying P-to-S converted phases by Rychert and Shearer (2009), who concluded that the LAB lies at 95 ± 4 km beneath Precambrian regions and 81 ± 2 km beneath "tectonically altered" regions. Whereas for Phanerozoic Europe our averages are close to Rychert and Shearer's, with central Europe displaying the Ps conversion at 70–80 km (Fig. 2 of Rychert and Shearer), for Precambrian Europe we differ by a factor of 2–3. The contention by Rychert and Shearer that the LAB beneath Precambrian regions lies at 95 ± 4 km is at odds with virtually all other geophysical determinations, at odds with petrological observations on xenolith samples from the mantle, and at odds with the existence of diamonds founds in kimberlites that must source from beneath the graphite-diamond stability field of around 160 km beneath cratons (Kennedy and Kennedy, 1976). That a seismic impedance boundary must exist at around 90–100 km beneath Precambrian regions is not questioned, but its attribution as the LAB is seriously in doubt. Possibly Rychert and Shearer have imaged the Hales discontinuity (Hales, 1969; Revenaugh and Jordan, 1991) rather than the LAB, highlighting the point that the attribution of a name to a boundary imaged geophysically or geochemically must be done with care.

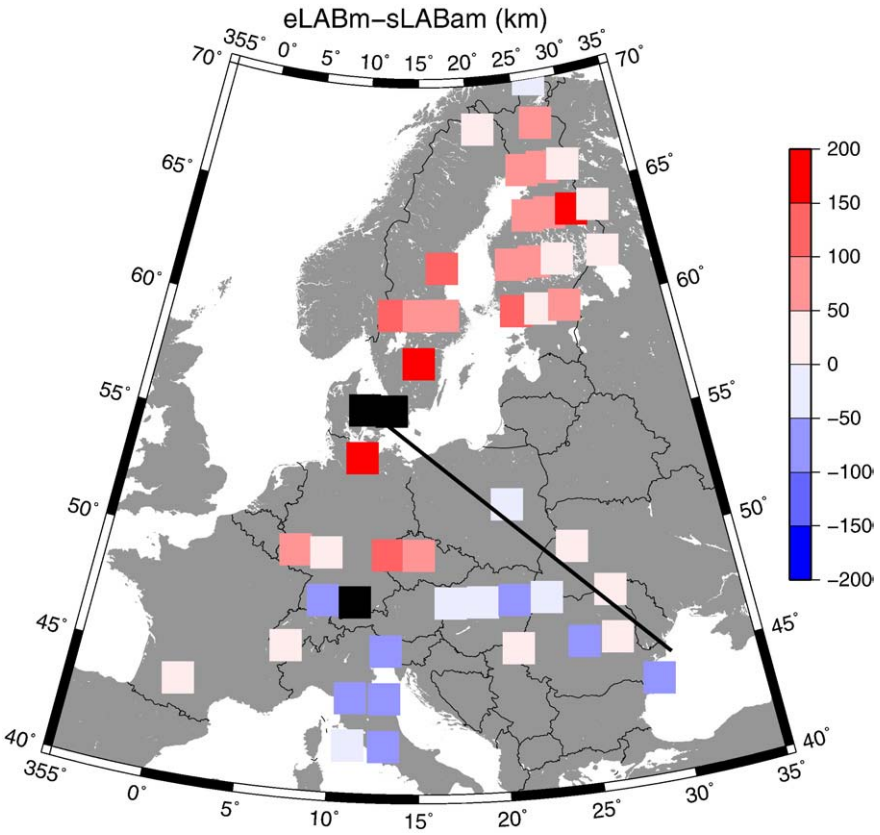

Fig. 17. The difference between the median smoothed eLABm and the sLABam estimates.

For Precambrian Europe the two seismic estimators of the LAB are in agreement, and are both relatively shallow at around 175 km, compared to the electrical LAB which has a far deeper averaged value of around 250 km. The body wave tomography model supports the eLAB results, suggesting that the TESZ boundary extends to around 250 km, with P-wave velocity in Precambrian Europe of >8.5 km/s, compared to Phanerozoic Europe where it is <8.5 km/s. Also, the lithospheric thickness map of Europe recently constructed from long period surface waves by Pasyanos (2010) shows a very sharp change across the TESZ from values less than 100 km for central Europe to values in excess of 260 km for the Baltic Shield.

Interpretation of high electrical conductivity is beset with contention (see above). It is a physical parameter that is amenable to accepting a wide variety of possible candidates given that a very small percentage (sub 1%) of some minor phase is sufficient to enhance conductivity by orders of magnitude. However, a far more powerful statement can be made in the *absence* of high conductivity — in such cases then there cannot be an interconnected conducting minor phase. Electrical conductivity is highly sensitive to water content (hydrogen diffusion, Karato, 1990, 2006) and partial melt (Jones, 1999), so in Precambrian Europe given the discordance between the eLAB and both sLAB results, with the eLAB being on average some 75 km deeper than the sLAB, both of these causes can be eliminated as the reason for the observed seismic anisotropy and RF interface. This would argue for the presence of a lowermost layer in the deepest part of cratonic lithosphere that is both dry and not molten but that is responding to shearing on the base of the lithosphere from plate driving forces leading to lattice preferred orientation (LPO) of olivine in the absolute plate motion (APM) direction. Such a model was previously proposed for the North American craton by Bokelman (Bokelmann, 2002a, b; Bokelmann and Silver, 2002).

For Phanerozoic Europe the situation is dramatically different and more complex. Statistically, the electrical (eLAB) and receiver function (sLABrf) LAB depths are in agreement in Phanerozoic Europe, but the anisotropy LAB (sLABa) is deeper. Here the evidence from the eLAB and sLABrf results is for a shallow LAB, around 90–95 km, below which the sLABrf results suggest is a layer about 40 km in thickness that is not responding to plate driving forces and has no LPO of olivine from APM, as the sLABrf results show an average around 135 km.

Arguably the most puzzling result from this comparison though of different physical properties of Europe's lithospheric mantle is the Trans-European Suture Zone (TESZ). All LAB estimates are consistent in giving evidence of a very sharp step-like change in the depth to the base of the lithosphere, consistent with many prior studies, but the "eLAB" estimates are all exceedingly deep (300–400 km) along the TESZ whereas the sLABa and sLABrf estimates do not exhibit such a thick root. This electrically very resistive root beneath the TESZ is also evident in recent analyses of extremely long periods from annual means of European observatory data (Dobrica and Demetrescu, 2009), effectively negating any attempt to ignore the TESZ eLAB results of Korja (2007) as due to either inappropriate modelling, non-uniform source effects, or other spurious phenomena. Again, the high resistivity does not permit any partial melt or any water to be present, thus effectively demonstrating that there is no electrical asthenosphere beneath the TESZ. It is worth noting that Gregersen et al. (2002) proposed that the asthenosphere is absent north of the TESZ along the TOR profile in southern Sweden based on P-wave travel time anomalies, again highlighting the difficulty in assigning a universal nature to the LAB.

Note that in the global compilation of Rychert and Shearer (Rychert and Shearer, 2009), the P-to-S conversion, that they attribute to the LAB, appears to be shallower north of the TESZ (~60 km) compared to south of it (70–80 km) (their Fig. 2). This is yet further confirmation that the P-to-S conversion being tracked by Rychert and Shearer is not everywhere validly interpreted as the LAB.

5. Conclusions

All three techniques used for identifying the lithosphere-asthenosphere boundary, namely magnetotellurics (eLAB) and receiver function and anisotropy seismological methods (sLABrf and sLABa), are qualitatively consistent, with thin lithosphere in Phanerozoic Europe and thick lithosphere in Precambrian Europe, with a sharp change at the Trans-European Suture Zone. This overarching result is supported by a new body wave tomographic model of Spakman (unpubl.) and by a recent long period surface wave model (Pasyanos, 2010).

The three differ though quantitatively, with the eLAB and sLABrf in agreement for central Phanerozoic Europe, and the sLABa and sLABrf in agreement for Precambrian Europe, but both being thinner than the eLAB and the LAB thickness from the recent surface wave model (Pasyanos, 2010). Where there are thick sedimentary basins, in northern Germany and the Pannonian Basin, the two seismological definitions, sLABa and sLABrf, are in agreement, to within error ($\pm$10 km) of each other.

For Precambrian Europe with its thick lithosphere, the sLABa and sLABrf definitions may be not the base of the lithosphere, but to a boundary within the lower lithosphere that is responding to shearing on the base of the lithosphere from plate driving forces (Bokelmann and Silver, 2002).

These quantitative differences between the three types of LAB estimates, though substantial in some regions, are not random. They each reflect some aspect(s) of the physical transition from the lithosphere to the asthenosphere, which need not be the same for different parameters, for the different age of the provinces, and of the same intensity relative to other discontinuities in the upper mantle. Classifying the differences does not define which of the methods is better or best, but contributes to improving our understanding of the nature of the lithosphere–asthenosphere boundary, which methods are suitable for detailed modelling of this most prominent transition in the upper mantle in different regions and to the interdisciplinary research of the “bottom” of the lithospheric plates and their structure.

What we have not addressed is the sharpness of the LAB. The SRF modelling suggests that the LAB is sharper beneath Central Europe than beneath the Precambrian platform of Eastern Europe (Geissler et al., 2010). Clearly, more detailed and focussed comparisons need to be made of the LAB and its sharpness across the whole of Europe and other locations where good seismological and electromagnetic data exist.

Acknowledgments

This paper is a result of the invitation to present a review of the European LAB at the 33rd International Geological Congress held in Oslo in August, 2008, and the authors wish to thank Sue O'Reilly for that invitation. The authors wish to thank the two reviewers, Prof. Marek Grad and an unknown reviewer, and Guest Editor Sue O'Reilly for their suggested improvements to the original version of this paper — their work has improved the final version.

The work of JP was supported by grant No. IAA300120709 of the Grant Agency of the Czech Academy of Sciences.

References

Amaru, M.L., Spakman, W., Villasenor, A., Sandoval, S., Kissling, E., 2008. A new absolute arrival time data set for Europe. Geophysical Journal International 173 (2), 465–472.

Anderson, D.L., 1995. Lithosphere, asthenosphere, and perisphere. Reviews of Geophysics 33 (1), 125–149.

Artemieva, I.M., 2009. The continental lithosphere: reconciling thermal, seismic, and petrologic data. Lithos 109 (1–2), 23–46.

Babuska, V., Plomerova, J., 1992. The lithosphere in central Europe — seismological and petrological aspects. Tectonophysics 207 (1–2), 141–163.

Babuska, V., Plomerova, J., 2006. European mantle lithosphere assembled from rigid microplates with inherited seismic anisotropy. Physics of the Earth and Planetary Interiors 158 (2–4), 264–280.

Babuska, V., Montagner, J.P., Plomerova, J., Girardin, N., 1998. Age-dependent large-scale fabric of the mantle lithosphere as derived from surface-wave velocity anisotropy. Pure and Applied Geophysics 151 (2–4), 257–280.

Bokelmann, G.H.R., 2002a. Convection-driven motion of the north American craton: evidence from P-wave anisotropy. Geophysical Journal International 148 (2), 278–287.

Bokelmann, G.H.R., 2002b. Which forces drive North America? Geology 30 (11), 1027–1030.

Bokelmann, G.H.R., Silver, P.G., 2002. Shear stress at the base of shield lithosphere. Geophysical Research Letters 29 (23), 4.

Constable, S., 2006. SEO3: a new model of olivine electrical conductivity. Geophysical Journal International 166 (1), 435–437.

Dobrica, V., Demetrescu, C., 2009. Large-scale European mantle electric structure as derived from ring current and geomagnetic observatory data, 11th IAGA Scientific Assembly Sopron, Hungary.

Eaton, D.W., Darbyshire, F., Evans, R.L., Grutter, H., Jones, A.G., Yuan, X.H., 2009. The elusive lithosphere–asthenosphere boundary (LAB) beneath cratons. Lithos 109 (1–2), 1–22.

Evans, R.L., Hirth, G., Baba, K., Forsyth, D., Chave, A., Mackie, R., 2005. Geophysical evidence from the MELT area for compositional controls on oceanic plates. Nature 437 (7056), 249–252.

Fasano, G., Vio, R., 1988. Fitting a straight line with errors on both coordinates. Newsletter of Working Group for Modern Astronomical Methodology 7, 2–7.

Fischer, K.M., Ford, H.A., Abt, D.L., Rychert, C.A., 2010. The lithosphere–asthenosphere boundary, annual review of Earth and Planetary Sciences. Annual Review of Earth and Planetary Sciences vol. 38, 551–575.

Geissler, W.H., Sodoudi, F., Kind, R., 2010. Thickness of the central and eastern European lithosphere as seen by S receiver functions. Geophysical Journal International 181 (604–634).

Ghods, A., Arkani-Hamed, J., 2000. Melt migration beneath mid-ocean ridges. Geophysical Journal International 140, 687–697.

Gregersen, S., Voss, P., Grp, T.O.R.W., 2002. Summary of project TOR: delineation of a stepwise, sharp, deep lithosphere transition across Germany–Denmark–Sweden. Tectonophysics 360 (1–4), 61–73.

Guterch, A., Grad, M., 2006. Lithospheric structure of the TESZ in Poland based on modern seismic experiments. Geological Quarterly 50 (1), 23–32.

Hales, A.L., 1969. A seismic discontinuity in the lithosphere. Earth and Planetary Science Letters 7, 44–46.

Hartigan, P.M., 1985. Algorithm AS217: computation of the dip statistic to test for unimodality. Applied Statistics 34 (3), 320–325.

Hartigan, J.A., Hartigan, P.M., 1985. The dip test of unimodality. The Annals of Statistics 13 (1), 70–84.

Heinson, G., 1999. Electromagnetic studies of the lithosphere and asthenosphere. Surveys in Geophysics 20 (3–4), 229–255.

Heit, B., Sodoudi, F., Yuan, X., Bianchi, M., Kind, R., 2007. An S receiver function analysis of the lithospheric structure in South America. Geophysical Research Letters 34 (14).

Hirth, G., Evans, R.L., Chave, A.D., 2000. Comparison of continental and oceanic mantle electrical conductivity: is the archean lithosphere dry. Geochemistry, Geophysics, Geosystems 1.

Huber, P.J., 1981. Robust Statistics. John Wiley, New York. 308 pp.

Jones, A.G., 1980. Geomagnetic induction studies in Scandinavia—I. Determination of the inductive response function from the magnetometer data. Journal of Geophysics 48, 181–194 (Zeitschrift fuer Geophysik).

Jones, A.G., 1988. Static shift of magnetotelluric data and its removal in a sedimentary basin environment. Geophysics 53 (7), 967–978.

Jones, A.G., 1999. Imaging the continental upper mantle using electromagnetic methods. Lithos 48 (1–4), 57–80.

Jones, A.G., Spratt, J., 2002. A simple method for deriving the uniform field MT responses in auroral zones. Earth Planets and Space 54 (5), 443–450.

Jones, A.G., Evans, R.L., Eaton, D.W., 2009. Velocity–conductivity relationships for mantle mineral assemblages in Archean cratonic lithosphere based on a review of laboratory data and application of extremal bound theory. Lithos 109, 131–143.

Karato, S., 1990. The role of hydrogen in the electrical conductivity of the upper mantle. Nature 347 (6290), 272–273.

Karato, S., 2006. Remote sensing of hydrogen in Earth's mantle, Water in Nominally Anhydrous Minerals. Reviews in Mineralogy & Geochemistry. Mineralogical Soc America, Chantilly, pp. 343–375.

Kawakatsu, H., Kumar, P., Takei, Y., Shinohara, M., Kanazawa, T., Araki, E., Suyehiro, K., 2009. Seismic evidence for sharp lithosphere–asthenosphere boundaries of oceanic plates. Science 324 (5926), 499–502.

Kennedy, C.S., Kennedy, G.C., 1976. Equilibrium boundary between graphite and diamond. Journal of Geophysical Research, Solid Earth 81 (14), 2467–2470.

Kennett, B.L.N., Engdahl, E.R., Buland, R., 1995. Constraints on seismic velocities in the Earth from travel times. Geophysical Journal of the Royal Astronomical Society 122, 108–124.

Korja, T., 2007. How is the european lithosphere imaged by magnetotellurics? Surveys in Geophysics 28 (2–3), 239–272.

Kumar, P., Kind, R., Hanka, W., Wylegalla, K., Reigber, C., Yuan, X., Woelbern, I., Schwintzer, P., Fleming, K., Dahl-Jensen, T., Larsen, T.B., Schweitzer, J., Priestley, K., Gudmundsson, O., Wolf, D., 2005. The lithosphere–asthenosphere boundary in the North-West Atlantic region. Earth and Planetary Science Letters 236 (1–2), 249–257.

Lahti, I., Korja, T., Kaikkonen, P., Vaittinen, K., Grp, B.W., 2005. Decomposition analysis of the BEAR magnetotelluric data: implications for the upper mantle conductivity in the Fennoscandian Shield. Geophysical Journal International 163 (3), 900–914.
Ledo, J., Jones, A.G., 2005. Upper mantle temperature determined from combining mineral composition, electrical conductivity laboratory studies and magnetotelluric field observations: application to the Intermontane belt, Northern Canadian Cordillera. Earth and Planetary Science Letters 236 (1–2), 258–268.
Li, X.Q., Yuan, X.H., Kind, R., 2007. The lithosphere–asthenosphere boundary beneath the western United States. Geophysical Journal International 170 (2), 700–710.
Maumus, J., Bagdassarov, N., Schmeling, H., 2005. Electrical conductivity and partial melting of mafic rocks under pressure. Geochimica Et Cosmochimica Acta 69 (19), 4703–4718.
Partzsch, G.M., Schilling, F.R., Arndt, J., 2000. The influence of partial melting on the electrical behavior of crustal rocks: laboratory examinations, model calculations and geological interpretations. Tectonophysics 317 (3–4), 189–203.
Pasyanos, M.E., 2010. Lithospheric thickness modeled from long-period surface wave dispersion. Tectonophysics 481 (1–4), 38–50.
Plomerova, J., Babuska, V., 2010. Long memory of mantle lithosphere fabric — European LAB constrained from seismic anisotropy. Lithos. doi:10.1016/j.lithos.2010.01.008.
Plomerova, J., Babuska, V., Vecsey, L., Kouba, D., Grp, T.O.R.W., 2002a. Seismic anisotropy of the lithosphere around the Trans-European Suture Zone (TESZ) based on teleseismic body-wave data of the TOR experiment. Tectonophysics 360 (1–4), 89–114.
Plomerova, J., Kouba, D., Babuska, V., 2002b. Mapping the lithosphere-asthenosphere boundary through changes in surface-wave anisotropy. Tectonophysics 358 (1–4), 175–185.
Plomerova, J., Babuska, V., Vecsey, L., Kozlovskaya, E., Raita, T., Sstwg, 2006. Proterozoic–Archean boundary in the mantle lithosphere of eastern Fennoscandia as seen by seismic anisotropy. Journal of Geodynamics 41 (4), 400–410.
Plomerova, J., Babuska, V., Kozovskaya, E., Vecsey, L., Hyvonen, L.T., 2008. Seismic anisotropy — a key to resolve fabrics of mantle lithosphere of Fennoscandia. Tectonophysics 462 (1–4), 125–136.
Praus, O., Pecova, J., Petr, V., Babuska, V., Plomerova, J., 1990. Magnetotelluric and seismological determination of the lithosphere–asthenosphere transition in central-Europe. Physics of the Earth and Planetary Interiors 60 (1–3), 212–228.
Pushkarev, P.Y., Ernst, T., Jankowski, J., Jozwiak, W., Lewandowski, M., Nowozynski, K., Semenov, V.Y., 2007. Deep resistivity structure of the Trans-European Suture Zone in central Poland. Geophysical Journal International 169 (3), 926–940.
Revenaugh, J., Jordan, T.H., 1991. Mantle layering from ScS reverberations: 3. The upper mantle. Journal of Geophysical Research 96 (B12), 19,781–19,810.
Romanowicz, B., 2009. The thickness of tectonic plates. Science 324 (5926), 474–476.
Rychert, C.A., Shearer, P.M., 2009. A global view of the lithosphere–asthenosphere boundary. Science 324 (5926), 495–498.
Rychert, C.A., Shearer, P.M., Fischer, K.M., 2010. Scattered wave imaging of the lithosphere–asthenosphere boundary. Lithos 120, 173–185.
Semenov, V.Y., Pek, J., Adam, A., Jozwiak, W., Ladanyvskyy, B., Logvinov, I.M., Pushkarev, P., Vozar, J., 2008. Electrical structure of the upper mantle beneath Central Europe: results of the CEMES project. Acta Geophysica 56 (4), 957–981.
Smirnov, M.Y., Pedersen, L.B., 2009. Magnetotelluric measurements across the Sorgenfrei–Tornquist Zone in southern Sweden and Denmark. Geophysical Journal International 176 (2), 443–456.
Sodoudi, F., Yuan, X., Liu, Q., Kind, R., Chen, J., 2006a. Lithospheric thickness beneath the Dabie Shan, central eastern China from S receiver functions. Geophysical Journal International 166 (3), 1363–1367.
Sodoudi, F., Kind, R., Hatzfeld, D., Priestley, K., Hanka, W., Wylegalla, K., Stavrakakis, G., Vafidis, A., Harjes, H.P., Bohnhoff, M., 2006b. Lithospheric structure of the Aegean obtained from P and S receiver functions. Journal of Geophysical Research, Solid Earth 111 (B12).
Sodoudi, F., Yuan, X., Kind, R., Heit, B., Sadidkhouy, A., 2009. Evidence for a missing crustal root and a thin lithosphere beneath the Central Alborz by receiver function studies. Geophysical Journal International 177, 733–742.
Tirone, M., Ganguly, J., Morgan, J.P., 2009. Modeling petrological geodynamics in the Earth's mantle. Geochemistry, Geophysics, Geosystems 10 (4), 28.
Varentsov, I.M., Sokolova, E.Y., Grp, B.W., 2003. Diagnostics and suppression of auroral distortions in the transfer operators of the electromagnetic field in the BEAR experiment. Izvestiya Physics of the Solid Earth 39 (4), 283–307.
Velikhov, Y.P., Zhamaletdinov, A.A., Belkov, I.V., Gorbunov, G.I., Hjelt, S.E., Lisin, A.S., Vanyan, L.L., Zhdanov, M.S., Demidova, T.A., Korja, T., Kirillov, S.K., Kuksa, Y.I., Poltanov, A.Y., Tokarev, A.D., Yevstigneyev, V.V., 1986. Electromagnetic studies on the Kola Peninsula and in Northern Finland by means of a powerful controlled source. Journal of Geodynamics 5, 237–256.
Wilde-Piorko, M., Swieczak, M., Grad, M., Majdanski, M., 2010. Integrated seismic model of the crust and upper mantle of the Trans-European Suture zone between the Precambrian craton and Phanerozoic terranes in Central Europe. Tectonophysics 481 (1–4), 108–115.
York, D., 1966. Least-squares fitting of a straight line. Canadian Journal of Physics 44 (5), 1079–1086.
York, D., 1969. Least squares fitting of a straight line with correlated errors. Earth and Planetary Science Letters 5, 320–324.
Yuan, X.H., Kind, R., Li, X.Q., Wang, R.J., 2006. The S receiver functions: synthetics and data example. Geophysical Journal International 165 (2), 555–564.